Chinese Chemical Letters 33 (2022) 3203–3206

Contents lists available at ScienceDirect

Chinese Chemical Letters

journal homepage: www.elsevier.com/locate/cclet

Achieving an electron transfer photochromic complex for switchable white-light emission

Qi Li, Wuji Wei, Zhenzhen Xue*, Ying Mu, Jie Pan, Jixiang Hu*, Guoming Wang

College of Chemistry and Chemical Engineering, Qingdao University, Qingdao 266071, China

ARTICLE INFO

Article history:
Received 20 August 2021
Revised 3 October 2021
Accepted 11 October 2021
Available online 16 October 2021

Keywords:
Charge separation
Electron transfer
Photochromism
Photogenerated radicals
White-light emission

ABSTRACT

Tuning white-light emission *via* free radicals is still a challenge in molecular-based functional materials. Herein, a new photoactive Zn^{2+} oxalate-based chain containing a polypyridine ligand was designed and synthesized with remarkably bifunctional photochromism and photo-actuated greenish white-light emission after UV, sunlight or Xe lamp light irradiation at room temperature. The photo-actuated coloration process was induced by the photogeneration of stable radicals originated from intermolecular electron transfers from oxalate components to the protonated polypyridine units, as demonstrated by UV–vis, IR, electron spin resonance and X-ray photoelectron spectra and magnetic measurements. Importantly, the on/off greenish white light emission (WLE) could be reversibly switched by generation and elimination of radicals *via* light irradiation and heat treatment, providing a feasible strategy for designing photo-switchable light emission diodes materials.

Molecule-based materials with external stimuli-responsive actuation, such as light, temperature, humidity and pressure, have attracted much attention and hold a great promise among various practical applications in the field of functional materials [1–12]. Especially, electron transfer photochromic architectures, with bistable states of different color and electronic forms, have been universally utilized in chemical switches, memories, molecular sensors and anti-counterfeiting devices [13–21]. *Via* incorporation of electron donor/acceptor ligands and metal ions, hybrid electron transfer photochromic complexes could be efficiently synthesized showing both the merits of organic and inorganic components [22–27]. In recent years, multiple properties including nonlinear optical properties, semiconductors, single molecular magnets, room temperature phosphorescence and proton conductivities have been achieved in this kind of photochromic complexes [28–36]. However, it is still a challenge for the combination of this photochromism with photoluminescence, in particular white light emission (WLE) simultaneously, due to the fact that typically photogenerated radicals just decreased the emission intensities of photoluminescence [37]. Photochromic materials possessing WLE performance may display fascinating application features in displays, optical switches and other optical devices [38–41].

In general, the WLE devices could be fabricated by the combination of the different emissions from separate chromophores or multiple components [42–46]. The problem lies that the distinct decay speeds of the respective phosphors could induce the gradual changes of emissions during practical application. Another effective method to produce WLE is directly synthesizing a single-component structure, doping different halide/lanthanide ions or encapsulating specific organic dyes into the metal-organic complexes [47–52]. In addition, the WLE of the single-component materials could be achieved *via* the alternation of temperature or excitation band [53–56], but it suffers from inconvenience to control the operating temperature or modulate different lasers. By contrast, utilizing room temperature single light irradiation to realize the WLE offers a promising route for the preparation of emitting solids and would probably simplify the fabrication procedure for the device application.

In this regard, the electron transfer photochromic materials with tunable photoluminescence may provide an opportunity to obtain WLE solids excited by a single light source under ambient conditions. In our previous work, a 1,3,5-tris(4-pyridyl)benzene (TPB) ligand was utilized to construct an electron transfer photochromic complex with tunable fluorescence/phosphorescence dual-emission [57]. This pyridine-derived molecule could be capable of an alternative component for the construction of photochromic complexes with WLE benefitting from the following aspects: (1) Free radicals could be simultaneously photogenerated in the protonating TPB ligands and further tuning photo responsive coloration as well as luminescence performance; (2) The photogenerated radicals could be alternatively stabilized by intermolec-

* Corresponding authors.
E-mail addresses: tsingtaoxue@163.com (Z. Xue), hujixiang@qdu.edu.cn (J. Hu).

https://doi.org/10.1016/j.cclet.2021.10.015
1001-8417/

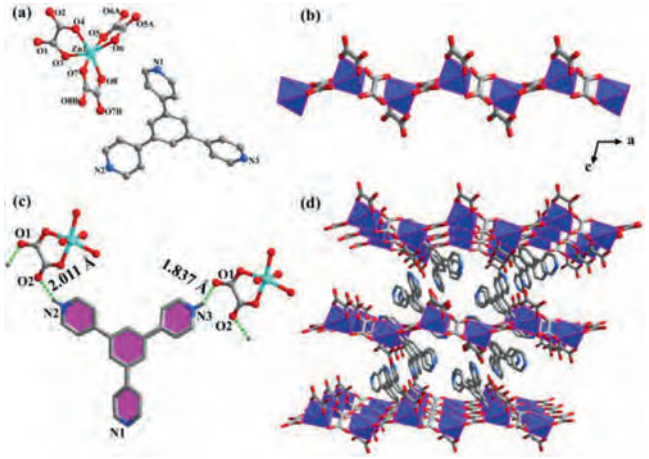

Fig. 1. Crystal structure of **1**. (a) The asymmetric unit; (b) The zinc oxolate chain; (c) H-bonding interactions between chelated oxalates and isolated TPB ligands; (d) Three-dimensional supramolecular structure. Atom legend: Zn, turquoise; N, blue; O, red; C, gray −40%. Polyhedral legend: [ZnO_6], light blue. Water molecules and part H atoms are omitted for clarity.

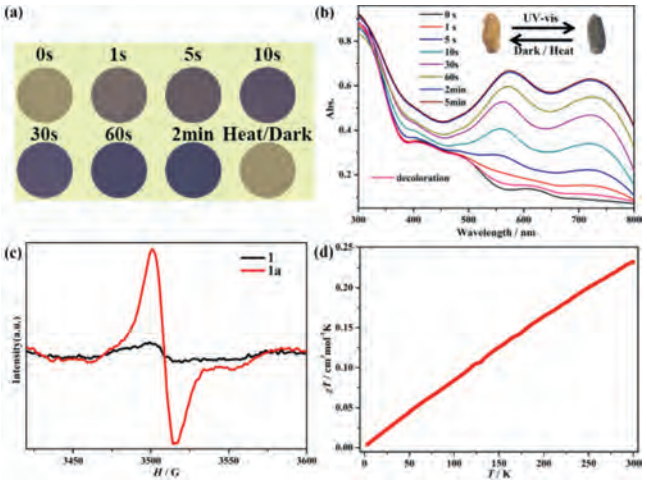

Fig. 2. (a) Photochromism of powder samples for compound **1**. (b) Time-dependent UV–vis spectra of **1**. Insert: Photochromism of crystal samples. (c) Solid state ESR spectra of **1** and **1a** under ambient conditions. (d) Temperature-dependent susceptibilities for **1a** under a dc field of 1000 Oe.

ular stacking interactions and quenched by heat treatment, enriching and improving the reversibly photochromic performance of the constructed materials; (3) The fluorescence/phosphorescence dual-emission property of this ligand offers a capacity for tuning WLE during coloration. Considering the above thoughts, introducing the electron-deficient TPB ligand with luminescence and phosphorescence dual-emission to the photochromic architectures could probably result in single-component WLE through the alternation of two emission bands in the presence of photogenerated radicals.

In this work, *via* self-assembly of TPB ligand, oxalic acid and $ZnSO_4{\cdot}7H_2O$, a new photochromic complex $[Zn(C_2O_4)_2]{\cdot}(H_2\text{-}TPB){\cdot}H_2O$ (**1**) showing an infinite chain was synthesized with interesting photoactive phenomenon. After Xe-lamp illumination, this compound underwent reversible photochromic behavior accompanied with the crystal color changed from claybank to charcoal gray, giving rise to the totally colored samples **1a**. The in-depth measured UV–vis, photoluminescent emission, electron spin resonance (ESR) and X-ray photoelectron spectra (XPS) and variable temperature magnetic measurements demonstrated that photogenerated radicals appeared with a ligand-to-ligand electron transfer from oxalate donors to TPB acceptors. Moreover, the greenish WLE could be readily achieved with 270 nm excitation *via* tuning the fluorescence/phosphorescence dual-emission behavior during photochromism. Interestingly, the emission color between blue and greenish white could be reversibly switched by generation and removal of radicals *via* light irradiation and heat treatment, providing a strategy for designing photoswitchable light emission diodes materials *via* electron transfer photochromism.

Complex **1** crystallizes in the triclinic $P\bar{1}$ space group and displays an infinite chain structure (Table S1 in Supporting information). The asymmetric unit contains one Zn^{2+}, two $C_2O_4^{2-}$, one protonated H_2-TPB^{2+} and one lattice water molecule (Fig. 1a). As shown in Fig. 1b, the Zn^{2+} center is connected with three discrete oxalates, with one of the oxalate anions chelating to the metal ion and the other two chelating/bridging two adjacent Zn^{2+} atoms, forming a one-dimensional chain along the *a* axis. The lengths of Zn−O bonds lengths are measured to be in the range of 2.064(2)–2.118(3) Å, with the O−Zn−O angels ranging from 78.32(10)° to 169.78(9)° (Table S2 in Supporting information). A continuous shape measurement indicates that the [ZnO_6] configuration is in a distorted octahedron (CShM = 1.504, Table S3 in Supporting information). It is worth noting that H-bonding interactions are formed between chelated oxalate O atoms and H atoms of TPB ligands, with the corresponding distances being within 1.837(1)–2.011(1) Å (Fig. 1c and Table S4 in Supporting information). The H-bonding interactions are beneficial for the electron transfer photochromic behavior for **1**. In this complex, neighboring chains are further connected by H-bonds with TPB anions and dissociative water molecules to form a three-dimensional supramolecular structure (Fig. 1d).

The stability of the compound **1** was firstly tested by thermogravimetric analysis (TGA). As shown in Fig. S1 (Supporting information), in the low temperature regions, there are three obvious weight loss steps in 30–150 °C, 215–240 °C and 265–295 °C (exp.: 2.70%, 9.02% and 26.95%, respectively), corresponding to the loss of one crystal water, one CO_2 molecule and the decomposition of oxalate ligands. As the temperature rises above 320 °C, the curve drops sharply, which is due to the decomposition of TPB ligands. Experimental powder X-ray diffraction (PXRD) of compound **1** was also performed before photochromism, and the curve in accordance with the simulated one from SCXRD data confirms the purity of the polycrystalline samples (Fig. S2 in Supporting information).

The photochromic behavior of **1** is performed with light irradiation at room temperature. Markedly, once being exposed to Xenon lamp (320–780 nm, 300 W), solid **1** presents an obvious color change from claybank to brown in just a few seconds and finally becomes dark blue over time (Fig. 2a). In addition, the single crystal color can also display the similar phenomenon during illumination (Fig. 2b, insert). Besides, this photochromism can also be induced by sunlight or UV light, showing a high sensitivity and a wide wavelength of light response. The decoloration process could be realized *via* putting the samples in the dark for 7 days or heating for 10 h. To explore its photochromic behavior, the time-dependent solid-state ultraviolet-visible (UV–vis) spectra of compound **1** are measured during light irradiation by Xenon lamp. As shown in Fig. 2b, two new absorption peaks centered at 560 nm and 735 nm appear and get stronger with the duration of light irradiation, implying the generation of $TPB^{\bullet}$ radicals. After decoloration, these characteristic peaks almost disappear and the sample returns to its initial state again, showing a reversible photoactivity of **1**. The unchanged crystal data, PXRD and IR spectra before and after light irradiation (Table S2, Figs. S2 and S3 in Supporting information) also exclude the photoinduced photolysis or isomerization, suggesting an electron transfer process in this photochromism.

Additionally, to confirm the photogenerated radicals, the electron spin resonance (ESR) spectra before and after irradiation have been studied at solid state with a frequency of 9.84 GHz. As depicted in Fig. 2c, a clearly sharp signal at $g = 2.003$ appears for **1a**, demonstrating the photogeneration of TPB$^{\bullet}$ radicals, which is consistent with the changes of the above UV–vis spectra. The small peak of radical signal before irradiation also suggests a high sensitivity to light for **1**. Furthermore, temperature-dependent susceptibilities for **1a** are measured between 300 K and 2 K under a direct current (dc) field of 1000 Oe (Fig. 2d). The χT value is 0.24 cm^3 K/mol at 300 K, suggesting the generation of relatively stable radicals. Then the χT values linearly decrease to nearly zero at 2 K, showing the temperature independent paramagnetism for the free radicals in **1a**.

XPS measurements were performed to provide deeper insight into the photochromic mechanism and electron transfer pathway. Compared with the spectrum before irradiation, the core-level spectrum of Zn^{2+} 2p shows negligible changes after irradiation, indicating that Zn centers do not contribute to photochromism and maintain its +2-valence state in the photodecomposition process (Fig. S4 in Supporting information). However, the positions of the major peaks in the C, O and N core-level spectra exhibit discernible variations before and after irradiation (Figs. S5–S7 in Supporting information). For C 1s, the fitted binding energies move from 284.67 and 285.97 eV to 284.80 and 287.03 eV after coloration. Also, the fitted O 1s peaks at 531.27 and 529.97 eV shift to 531.65 and 530.25 eV with higher binding energies after irradiation, suggesting C and O atoms in oxalate units lose electrons during irradiation and may be decarboxylated after light irradiation. Meanwhile, the N 1s peaks at 398.97 and 400.95 eV shift to lower binding energies of 398.85 and 400.75 eV after irradiation, indicating N atoms in TPB ligands accept electrons, and consistent with other reported electron transfer photochromic materials [58]. The above XPS analyses indicate that the photochromism of **1** originated from the photogeneration of radicals should be caused by electron transfer process from electron-rich oxalate units to electron-deficient TPB components.

For further exploring the light-induced coloration process, *in-situ* time-dependent photoluminescent (PL) emission spectra for **1** are also studied at ambient conditions. The photoluminescent emission spectrum of the TPB ligand has been confirmed in our previous work [57], accompanied with the fluorescence and phosphorescence properties. For compound **1**, a sharp emission peak centered at 380 nm appears after the powder samples are excited by 270 nm light, which should be ascribed to the TPB ligands (Fig. 3 and Fig. S8 in Supporting information). The lifetime of this fluorescence is fitted as 1.25 ns (Fig. S9 in Supporting information). As the illumination time increases, the peak intensity clearly decreases, indicating the TPB radical analogs gradually generate and induce the fluorescence quenching. Interestingly, a broad peak centered at 550 nm appears and becomes stronger in intensity upon irradiation, indicating the enhanced RTP behavior. This phosphorescence phenomenon is confirmed by the lifetime (26.51 ms) of delayed PL spectra of **1** excited at 270 nm (Fig. S10 in Supporting information), as demonstrated in our previous work [57]. This anomaly should be due to the increased radical absorption band and the delocalization of photogenerated radicals in the π-conjugated TPB ligands, which further induces variations in the torsion angles and intermolecular C–H···π stacking interactions in TPB ligands (Fig. S11 in Supporting information) [58,59]. After decoloration, the intensity of fluorescence and phosphorescence returns to the initial state (Fig. S8), indicating that the photochromism and photoluminescence of compound **1** is switchable and reversible under ambient conditions. Meanwhile, the reversibility and fatigue resistivity could be further confirmed by *in-situ* fluorescence spectra *via* alternative light irradiation and heat treatment, and the coloration/decoloration process for **1** could be cycled at least fifteen times (Fig. S12 in Supporting information).

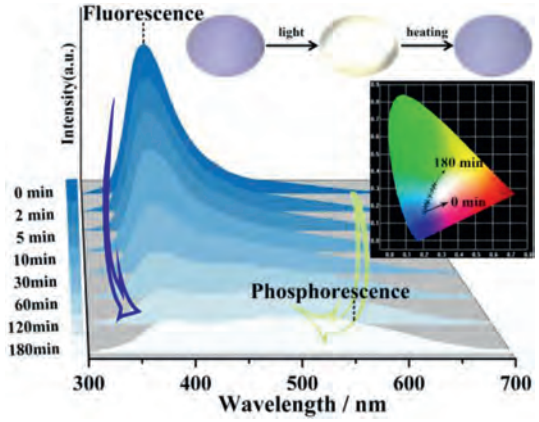

Fig. 3. Time-dependent photoluminescent spectra of **1**. Insert: Photo-excited images under 270 nm irradiation during reversible photochromism; Chromaticity coordinates of **1** at different irradiation time ($\lambda_{ex} = 270$ nm, 150 W; CIE = (0.20, 0.16) for 0 min, (0.21, 0.19) for 2 min, (0.22, 0.21) for 5 min, (0.23, 0.23) for 10 min, (0.24, 0.26) for 30 min, (0.25, 0.29) for 60 min, (0.26, 0.31) for 120 min, (0.27, 0.33) for 180 min).

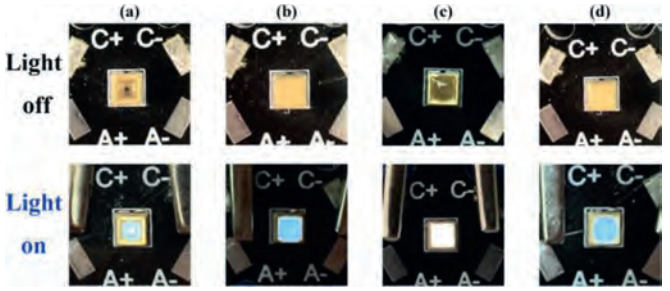

Fig. 4. (a) Photos of commercial 270 nm UV LED in light-off and light-on states. Photos of commercial 270 nm UV LED covered by thin layer of (b) sample **1**, (c) **1a** and (d) after decoloration in light-off and light-on states.

It can be seen from Fig. S8 that the fluorescence intensity at 380 nm drops dramatically by 83.92% when exposing the samples to 270 nm light for 3 h, while the phosphorescence intensity at 550 nm increases by 211.02% of the initial value. Interestingly, accompanied with the reversible photochromism between claybank and dark blue, the photoluminescence emission color can be changed from blue to white with the duration of light irradiation. The luminescence colors could be quantified by the CIE coordinates based on the 1931 CIE chromaticity diagram [60], with the (x, y) values being (0.20, 0.16) and (0.27, 0.33) before and after irradiation, respectively (Fig. 3 and Fig. S8). Notably, the value after coloration is close to the pure white light (0.33, 0.33). The photoluminescent intensity changes lead to the transition from blue light to greenish white light emission of compound **1**. For the first time, the reversibly controlled WLE behavior *via* tunable luminescent and phosphorescent dual emission induced by continuous single light irradiation is achieved in the electron transfer photochromic materials.

As is well known, the white light emitting diodes (WLEDs) possess broad application prospects and great commercial values in the solid-state lighting and displaying field. The photochromic and WLEDs phenomenon mentioned above enlighten us to explore practical applications for compound **1**. The photos of commercial 270 nm UV LED in light-off and light-on states are firstly shown in Fig. 4a. Then the claybank thin layer made from the mixed powder sample of **1** and transparent resins are coated on the surface of a commercial 270 nm UV LED (Fig. 4b and Fig. S13). When the

LED turns on, the sample emits a blue light. After coloration for **1a**, the fabricated LED shows a bright WLE in the light-on state with the color of thin layer being changed to charcoal gray (Fig. 4c). After decoloration, the color of layer itself and photoluminescence relax back to claybank and blue respectively (Fig. 4d). As mentioned above, compound **1** can maintain coloration/decoloration process for at least 15 times, suggesting this photochromic compound could be regarded as promising phosphor materials for practical lighting applications.

In conclusion, a zinc oxalate-based chain complex with photochromism, photo-enhanced RTP and photo-controlled WLE properties was synthesized under the assembly of a fluorescence and phosphorescence dual emission TPB ligand. The compound undergoes the electron transfer process from oxalate groups to TPB ligands upon light irradiation, which is confirmed by UV–vis, ESR, IR, XPS spectra and magnetic analysis. Meanwhile, the photogenerated radicals could lead to the changes in electronic and crystal structures of the title compound, leading to the enhanced RTP behavior. The reversible photoluminescence between blue and greenish white light emission was innovatively achieved in this photochromic zinc oxalate chain system by generation and removal of radicals using external stimuli. This study could serve as a representative architecture for rational design of novel photochromic materials with photoswitchable WLE, opening a new way for developing stimuli-switchable white light-emitting diodes.

Declaration of competing interest

The authors declare that they have no known competing financial interests or personal relationships that could have appeared to influence the work reported in this paper.

Acknowledgments

This work was supported by the National Natural Science Foundation of China (Nos. 21901133, 22171155 and 22071126) and the State Key Laboratory of Fine Chemicals (No. KF 1905).

Supplementary materials

Supplementary material associated with this article can be found, in the online version, at doi:10.1016/j.cclet.2021.10.015.

References

[1] E. Coronado, E.G. Mínguez, Chem. Soc. Rev. 42 (2013) 1525–1539.
[2] M. Karimi, A. Ghasemi, Z.P. Sahandi, et al., Chem. Soc. Rev. 45 (2016) 1457–1501.
[3] C.G. Palivan, R. Goers, A. Najer, et al., Chem. Soc. Rev. 45 (2016) 377–411.
[4] O. Sato, Nat. Chem. 8 (2016) 644–656.
[5] Y.S. Meng, T. Liu, Acc. Chem. Res. 52 (2019) 1369–1379.
[6] C.C. Ko, V.W.W. Yam, Acc. Chem. Res. 51 (2018) 149–159.
[7] R. Usui, K. Yamamoto, H. Okajima, et al., J. Am. Chem. Soc. 142 (2020) 10132–10142.
[8] Q. Liu, J.X. Hu, Y.S. Meng, et al., Angew. Chem. Int. Ed. 60 (2021) 10537–11541.
[9] Y. Xu, M. Tian, H. Zhang, et al., Chin. Chem. Lett. 29 (2018) 1093–1097.
[10] L. Tu, Y. Xu, Q. Ouyang, et al., Chin. Chem. Lett. 30 (2019) 1731–1737.
[11] J.H. Qin, H. Zhang, P. Sun, et al., Dalton Trans. 49 (2020) 17772–17778.
[12] J.H. Qin, Y.D. Huang, Y. Zhao, et al., Inorg. Chem. 58 (2019) 15013–15016.
[13] M.H. Li, M.H. You, M.J. Lin, Dalton Trans. 50 (2021) 4959–4966.
[14] B. Xia, Q. Gao, Z.P. Hu, et al., Research 2021 (2021) 5490482.
[15] Q. Sui, X.T. Ren, Y.X. Dai, et al., Chem. Sci. 8 (2017) 2758–2768.
[16] J. Zhang, Z. Yao, S. Liao, J. Dai, Z. Fu, J. Mater. Chem. A 1 (2013) 4945–4948.
[17] J.J. Liu, Dyes Pigments 163 (2019) 496–501.
[18] J.K. Sun, X.D. Yang, G.Y. Yang, J. Zhang, Coord. Chem. Rev. 378 (2019) 533–560.
[19] W. Huang, H. Yang, Z. Hu, et al., Adv. Healthc. Mater. 10 (2021) 2101003.
[20] Y. Sun, F. Ding, Z. Chen, et al., PNAS 116 (2019) 16729–16735.
[21] P. Wang, H. Yang, C. Liu, et al., Chin. Chem. Lett. 32 (2021) 168–178.
[22] L. Liu, Q. Liu, R. Li, M.S. Wang, G.C. Guo, J. Am. Chem. Soc. 143 (2021) 2232–2238.
[23] J. Wu, C. Tao, Y. Li, et al., Chem. Sci. 5 (2014) 4237–4241.
[24] S.L. Li, M. Han, Y. Zhang, et al., J. Am. Chem. Soc. 141 (2019) 12663–12672.
[25] L. Li, Z.M. Tu, Y. Hua, et al., Inorg. Chem. Front. 6 (2019) 3077–3082.
[26] A.J. Liu, F. Xu, S.D. Han, et al., Cryst. Growth Des. 20 (2020) 7350–7355.
[27] Q. Li, Q. Zhang, W.J. Wei, et al., Chem. Commun. 57 (2021) 4295–4298.
[28] J.X. Hu, X.F. Jiang, Y.J. Ma, et al., Sci. China Chem. 64 (2021) 432–438.
[29] H.Y. Li, H. Xu, S.Q. Zang, T.C.W. Mak, Chem. Commun. 52 (2016) 525–528.
[30] Q. Zhang, J.X. Hu, Q. Li, et al., Chin. Chem. Lett. 32 (2022) 1417–1421.
[31] G.E. Wang, G. Xu, N.N. Zhang, et al., Angew. Chem. Int. Ed. 58 (2019) 2692–2695.
[32] Y.J. Ma, J.X. Hu, S.D. Han, J. Pan, J.H. Li, G.M. Wang, J. Am. Chem. Soc. 142 (2020) 2682–2689.
[33] J.Z. Liao, L. Meng, J.H. Jia, et al., Chem. Eur. J. 24 (2018) 10498–10502.
[34] Q. Zhang, W.J. Wei, Q. Li, et al., Sci. China Chem. 64 (2021) 1170–1176.
[35] P.X. Li, Z.X. Xie, A.P. Jin, J. Li, G.C. Guo, Chem. Commun. 56 (2020) 14689–14692.
[36] W. Yang, H.R. Tian, J.P. Li, et al., Chem. Eur. J. 22 (2016) 15451–15457.
[37] M. Bälter, S. Li, M. Morimoto, et al., Chem. Sci. 7 (2016) 5867–5871.
[38] H. Lu, J. Xie, X.Y. Wang, et al., Nat. Commun. 12 (2021) 2798.
[39] F. Gu, C. Zhang, X. Ma, Rapid Commun. 40 (2019) 1800751.
[40] Z.Z. Xue, X.D. Meng, X.Y. Li, et al., Inorg. Chem. 60 (2021) 4375–4379.
[41] C. Sun, Y.H. Guo, Y. Yuan, et al., Inorg. Chem. 59 (2020) 4311–4319.
[42] W. Liu, D. Banerjee, F. Lin, J. Li, J. Mater. Chem. C 7 (2019) 1484–1490.
[43] N. Sun, B. Yan, Phys. Chem. Chem. Phys. 19 (2017) 11708.
[44] S. Wang, Y. Yao, Z. Wu, Y. Peng, L. Li, J. Luo, J. Mater. Chem. C 6 (2018) 12267–12272.
[45] A. Yangui, R. Roccanova, T.M. McWhorter, et al., Chem. Mater. 31 (2019) 2983–2991.
[46] G.M. Mileo, T. Kundu, R. Semino, et al., Chem. Mater. 29 (2017) 7263–7271.
[47] Z.W. Zhuang, C.D. Peng, G.Y. Zhang, et al., Angew. Chem. Int. Ed. 56 (2017) 14411–14416.
[48] M.S. Wang, S.P. Guo, Y. Li, et al., J. Am. Chem. Soc. 131 (2009) 13572–13573.
[49] D. Zhang, Z.Z. Xue, J. Pan, et al., Cryst. Growth Des. 18 (2018) 7041–7047.
[50] Y. Cui, T. Song, J. Yu, Y. Yang, Z. Wang, G. Qian, Adv. Funct. Mater. 25 (2015) 4796–4802.
[51] Z. Wang, C.Y. Zhu, J.T. Mo, et al., Angew. Chem. Int. Ed. 58 (2019) 9752–9757.
[52] T. Jiang, X. Wang, J. Wang, G. Hu, X. Ma, ACS Appl. Mater. Inter. 11 (2019) 14399–14407.
[53] J. Miao, Y. Nie, Y. Li, et al., J. Mater. Chem. C 7 (2019) 13454–13460.
[54] G.E. Wang, G. Xu, M.S. Wang, et al., Chem. Sci. 6 (2015) 7222–7226.
[55] M. Yu, P. Zhang, B.P. Krishnan, et al., Adv. Funct. Mater. 28 (2018) 1804759.
[56] W.J. Wei, Y. Mu, L. Wei, J.X. Hu, G.M. Wang, Inorg. Chem. 60 (2021) 108–114.
[57] C.J. Zhang, Z.W. Chen, R.G. Lin, et al., Inorg. Chem. 53 (2014) 847–851.
[58] M.H. You, M.H. Li, Y.M. Di, Y.W. Wang, M.J. Lin, Dyes Pigments 173 (2020) 107943–107951.
[59] H. Liu, Z.X. Xie, J. Lu, et al., Dyes Pigments 181 (2020) 108441–108446.
[60] J. Bu, K. Watanabe, H. Hayasaka, K. Akagi, Nat. Commun. 5 (2014) 3799.